J. Fluid Mech. (2004), *vol.* 499, *pp.* 257–276. © 2004 Cambridge University Press
DOI: 10.1017/S0022112003007171 Printed in the United Kingdom

Continuously stratified exchange flow through a contraction in a channel

By ANDREW McC. HOGG AND PETER D. KILLWORTH

James Rennell Division, Southampton Oceanography Centre, European Way, Southampton SO14 3ZH, UK

(Received 19 December 2002 and in revised form 29 May 2003)

Existing solutions for exchange flow through straits rely upon the decomposition of the flow into a finite number of layers which have constant density. In this paper we provide a solution to inviscid steady exchange flow between continuously stratified reservoirs, where it is assumed that the flow in each direction is independently self-similar. The solution requires knowledge only of the two reservoir stratifications and an imposed net barotropic throughflow. The solution includes regions of stagnant fluid which separate two counter-flowing, stably stratified layers, with the provision that the two active layers may touch at no more than one point. Comparison of the theoretical solution with numerical simulations indicates that the assumption of self-similarity is reasonable, and that the disparity between the theoretical and simulated flows can be attributed to the inclusion of diffusion and viscosity in the numerical model.

1. Introduction

Density-driven exchange flow through a channel connecting two reservoirs occurs in many geophysical systems, in particular between ocean basins, between semi-enclosed seas and the open ocean, and at the mouth of estuaries. Such flows occur on scales too small for numerical models of, for example, ocean circulation to resolve the dynamics. Therefore parameterization of exchange flows is desirable in such models. To first order, a solution for bi-directional exchange can be obtained by assuming a two-layer structure in the flow. Using this formulation it is possible to derive an upper bound for the flux of volume and mass through the channel, and to predict layer heights and velocities which qualitatively represent observations from the field and the laboratory.

The two-layer approach to exchange flows is based on internal hydraulics, and was first explored by Wood (1970), whose solution has been enhanced by several other authors (Armi 1986; Armi & Farmer 1986; Lawrence 1990; Dalziel 1991). The two-layer hydraulic solution can be applied to steady flow through a channel which separates two reservoirs which have homogeneous but different densities, provided that the fluid is inviscid, hydrostatic, non-rotating and incompressible. The solution relies upon the formation of control points in the flow (Wood 1968) where the speeds of long interfacial waves are zero (Dalziel 1991). For a channel which has a flat bottom and varies in width to form a simple contraction, the maximum flux occurs when two hydraulic controls are present, one of which will be at the minimum width of the contraction (Armi & Farmer 1987). The solution can then be specified globally from knowledge of reservoir densities and conditions at the control points.

The hydraulic solution can be used to give a first-order prediction of flow through a channel. However, geophysical flows are invariably more complicated than the

https://doi.org/10.1017/S0022112003007171 Published online by Cambridge University Press

two-layer theory. Modifications or corrections to the theory have been formulated to include effects which are explicitly ignored by the two-layer solution, such as time-dependence (Helfrich 1995), non-hydrostatic effects (Zhu & Lawrence 1998), mixing (Winters & Seim 2000; Hogg, Ivey & Winters 2001) and the influence of stable stratification in the reservoirs (Killworth 1992; Engqvist 1996; Lane-Serff, Smeed & Postlethwaite 2000). It is the last case with which we are concerned here.

Continuously stratified internal hydraulics was investigated by Killworth (1992) for the case of uni-directional flow using density coordinates. In appendix A of that paper it was demonstrated that if inviscid bi-directional exchange between stratified reservoirs were to occur, then the vertical position $z(x, \rho_c)$ of the streamline dividing the two counter-flowing regions is given by

$$z(x, \rho_c) = z_0(\rho_c), \tag{1.1}$$

where z_0 is a constant. In other words this streamline can only occupy one position in the vertical: it must be flat everywhere. This result breaks down in two cases: first, when the density coordinates are discontinuous (that is, when the vertical gradient in density is zero) and second, when there is a discontinuity in density at the dividing streamline. The implication of this result is that solutions to bi-directional stratified exchange flow occur either when there is a region of zero density gradient at the zero velocity streamline, or if the zero velocity streamline is coincident with a discontinuity in the density profile. Fuller details of the possible behaviour at the dividing streamline are given in the Appendix of this paper; a desire to understand which solution would occur partly led to this work.

Other attempts to include stratification in the exchange flow solution use multi-layer formulations stemming from Baines' (1988) description of stratified flow over an obstacle. Engqvist (1996) applied this multi-layer formulation to bi-directional exchange flows through a contraction, by dividing the multiple layers into left- and right-flowing groups. If the two groups of active layers are separated by a central layer which has zero velocity, then the problem can be solved. The central stagnant layer has the effect of decoupling the two groups of layers so that control conditions for each group of layers can be solved independently. The result is that each group of layers independently satisfies Wood's (1968) criteria for control of the selective withdrawal problem.

It is straightforward to show that as the number of layers in Engqvist's solutions tends to infinity, his analysis tends to Killworth's (1992) continuous solution, and the thickness of the stagnant layer becomes vanishingly small. In such a case, it is unclear whether the upper and lower active layers could remain independent. Thus we assume that Engqvist's solution can only be applied to cases where the reservoir stratifications allows a stagnant layer to form. More general multi-layer solutions have been investigated, and a three-layer exchange flow solution is now available (Smeed 2000; Lane-Serff *et al.* 2000). These studies include a complete interpretation of hydraulic control of the internal modes, and allows for flows which are subcritical with respect to the first internal wave mode, but supercritical with respect to the second mode.

There have been very few numerical or laboratory investigations into the nature of continuously stratified exchange flows. Armi & Williams (1993) looked at uni-directional stratified flow through a contraction. They noted that the flow was self-similar and could be well-described by Wood's (1968) solution, and also remarked upon the presence of stagnant regions of the flow.

https://doi.org/10.1017/S0022112003007171 Published online by Cambridge University Press

Stratification plays an important role in oceanic and geophysical flows. However, there is no general solution for exchange flow between stratified reservoirs; in particular, there is no theory available for how the streamline (or density contour) which divides the left- and right-going flow is selected, as a function of the reservoir stratifications and the net barotropic exchange between the reservoirs.

Motivated by the result of Killworth (1992) we have investigated the problem of flow through a flat-bottomed contracting channel using analytical techniques (§ 2) and a two-dimensional numerical model (§ 3). In short, we propose that the addition of stratification to this problem can yield simplifications to the two-layer hydraulic solution. We extend Engqvist's (1996) layered solution (in which a stagnant region separates two active layers) to continuously stratified flow. In addition we show a solution where the two active layers are allowed to make contact at one point. We test this theory against the numerical model, and show results in § 4.

2. Analytical model

2.1. *The selective withdrawal problem*

We start by revisiting the derivation of selective withdrawal of an inviscid fluid from a stratified reservoir which was originally due to Wood (1968); see also Yih (1969), Benjamin (1981) and Armi & Williams (1993). For this analysis we confine ourselves to the consideration of one layer where the reservoir density profiles and channel shape are known. The linear Bernoulli function for a Boussinesq fluid is written

$$B(x, z) = \frac{p + \rho g z}{\rho_0}, \tag{2.1}$$

where x is the horizontal coordinate, z denotes height, g acceleration due to gravity, ρ density, ρ_0 the reference density and p pressure. Define η, the upstream height coordinate which follows streamlines (so that in the reservoir $z = \eta$), and note that density conservation implies that $\rho = \rho(\eta)$ only. (We use the slightly more awkward upstream coordinate rather than density coordinates to ease potential difficulties if the vertical density gradient vanishes.) Conservation of energy along a streamline is then simply

$$\frac{\partial}{\partial x}\left(\tfrac{1}{2}u^2 + B\right) = 0, \tag{2.2}$$

where u is horizontal velocity. Equivalently, we can integrate with respect to x to give

$$\tfrac{1}{2}u^2 + B = B_\infty, \tag{2.3}$$

where $B_\infty(\eta)$ is the Bernoulli function in the upstream reservoir (which is assumed to be infinitely wide so that $u = 0$ there). The hydrostatic relation is applied under the assumption that the channel width varies slowly so that vertical velocities are small, giving

$$B_\eta = \frac{g z \rho_\eta}{\rho_0}, \tag{2.4}$$

which can be obtained from differentiation of (2.1). In particular,

$$B_{\infty\eta} = \frac{g \eta \rho_\eta}{\rho_0} \tag{2.5}$$

means that apart from some unknown barotropic addition, uniform with depth, $B_\infty(\eta)$ is known if the upstream stratification $\rho(\eta)$ is known.

https://doi.org/10.1017/S0022112003007171 Published online by Cambridge University Press

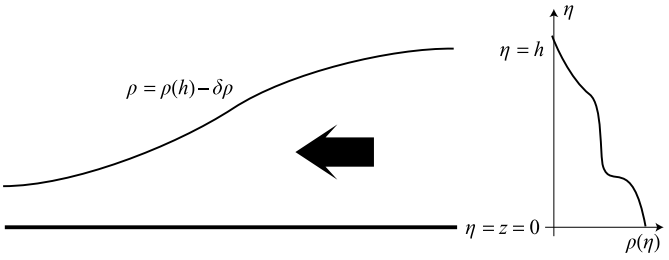


FIGURE 1. Schematic of one-layer flow along a flat-bottomed contracting channel. Reservoir stratification $\rho(\eta)$ is known, and the flowing region is bounded above by the $\eta = h$ streamline. Above the layer, fluid is stagnant with density $\rho(h) - \delta\rho$.

Conservation of volume along a streamline can be written, following Wood (1968),

$$\frac{\partial}{\partial x}(ubz_\eta) = 0, \tag{2.6}$$

where $b(x)$ is the channel width. This gives the flux Q along a streamline,

$$ubz_\eta = Q(\eta). \tag{2.7}$$

Equations (2.3) and (2.7) allow us to solve the selective withdrawal problem subject to the appropriate boundary conditions.

These equations are now applied to the specific case shown in figure 1. The boundary conditions on the flowing layer include a solid surface on the lower boundary where $z = 0$, giving

$$B_\eta(0) = 0, \tag{2.8}$$

from (2.4). There is a free upper surface with a density jump $\delta\rho$, so that (2.1) and (2.4) allow us to write

$$B(h) = \frac{\delta\rho B_\eta(h)}{\rho_\eta(h)}, \tag{2.9}$$

where h is the height at which withdrawal occurs in the upstream reservoir. This condition also applies to B_∞. We now assume that flow within the layer is self-similar (Wood 1968), or in other words the height and energy of a streamline can be separated into x- and η-dependent parts:

$$z(x, \eta) = \alpha(x)\eta, \tag{2.10}$$

and

$$B(x, \eta) = \alpha(x)(B_\infty(\eta) + C\rho + D), \tag{2.11}$$

where the functions $C(x)$ and $D(x)$ have been included for generality. These functions are derived from the above boundary conditions, and it can be shown that when B_∞ matches the boundary conditions, then so will B, giving $C = D = 0$, so that

$$B(x, \eta) = \alpha(x)B_\infty(\eta). \tag{2.12}$$

The factor α describes the reduction in height of a streamline from the upstream reservoir conditions.

The assumption of self-similarity allows us to write down a solution to this problem. The horizontal velocity u can be deduced from (2.3),

$$u = (2B_\infty(1 - \alpha))^{1/2}, \tag{2.13}$$

https://doi.org/10.1017/S0022112003007171 Published online by Cambridge University Press

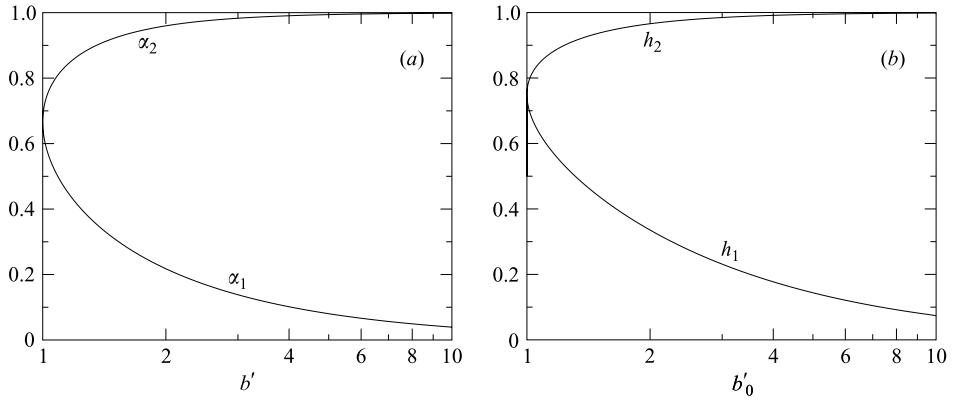


FIGURE 2. (*a*) The roots of $\alpha(b')$ given by (2.16). (*b*) The relative values for layer height given by (2.23).

and substituted into (2.7) to obtain

$$b(x)\alpha(x)(1-\alpha(x))^{1/2} = \frac{Q(\eta)}{(2B_\infty(\eta))^{1/2}}. \tag{2.14}$$

The left-hand side of (2.14) depends only upon x, while the right-hand side is a function of η, implying that both sides are constant. As is customary with controlled flows, we take the x-derivative of (2.14) to give

$$\frac{1}{b}\frac{\mathrm{d}b}{\mathrm{d}x} = \frac{1}{\alpha}\frac{\mathrm{d}\alpha}{\mathrm{d}x}\left(\frac{3\alpha-2}{2(1-\alpha)}\right). \tag{2.15}$$

When there is a minimum in $b(x)$, the solution can only be continuous when either $\mathrm{d}\alpha/\mathrm{d}x = 0$ or $\alpha = 2/3$. The latter case was defined by Wood (1968) as a point of hydraulic control. When conditions at this point are known, $\alpha(x)$ can be evaluated at any point in the channel, giving the velocity and density everywhere provided that the withdrawal height h is known. To do this, we note that the left-hand side of (2.14) may be written

$$b'\alpha(1-\alpha)^{1/2} = \frac{2}{3^{3/2}}, \tag{2.16}$$

where $b' = b/b_{min}$ is the non-dimensional width of the channel. Thus $\alpha = \alpha(b')$, and the two values of α predicted by (2.16) are shown in figure 2(*a*) as functions of b'.

2.2. *Application of self-similar flow to bi-directional exchange*

We now apply Wood's self-similar solution to exchange flows, where we have two stably stratified reservoirs at either end of a channel which has a simple minimum in width. It should be noted that although self-similarity has been observed in unidirectional flows, there is no *a priori* reason to suspect that the self-similarity condition is sufficiently strong to apply in all cases. Nonetheless we proceed with the intention of demonstrating that there are two distinct solutions for exchange flows in which the flow is self-similar, and that these solutions are viable.

The two cases considered are depicted in figure 3. In both examples we allow for two active layers flowing in opposite directions, and use two upstream vertical coordinates (η_1 for the upper layer, and η_2 for the lower layer), where the upper-layer coordinate has been inverted, which involves obvious sign changes in the algebra. The

https://doi.org/10.1017/S0022112003007171 Published online by Cambridge University Press

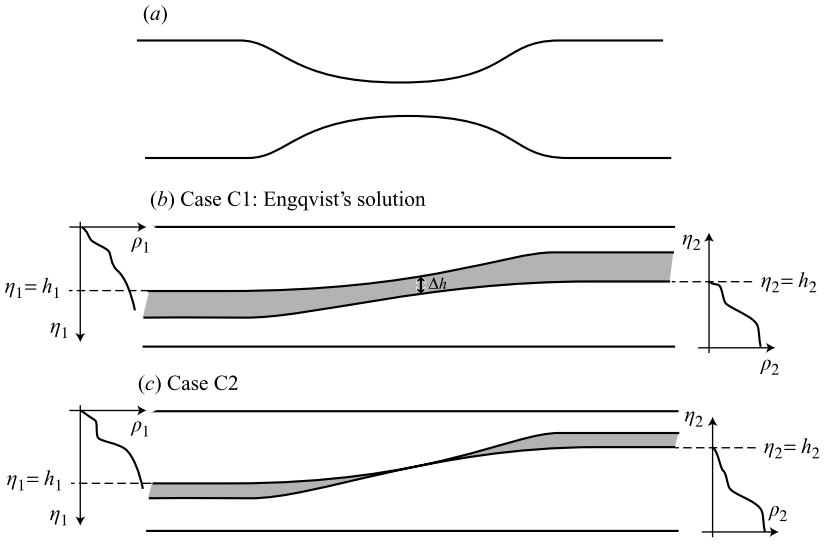


FIGURE 3. Schematic of stratified exchange flow. (*a*) Contracting channel in plan view. (*b*) Case C1: Engqvist's solution for two decoupled layers separated by a minimum distance of Δh. (*c*) Case C2: solution where flowing layers touch at one (and only one) point. In both cases upstream stratification for each layer, and upstream height coordinate are known.

first scenario (case C1, figure 3*b*) is simply the continuous extension of the layered solution proposed by Engqvist (1996), and we therefore refer to it as Engqvist's solution. In this solution there are two active layers which are divided by a stagnant, or inactive, region in which we assume that vertical gradients of both velocity and density are zero. At some point in the channel the stagnant region has a minimum thickness which we call Δh, and note that for this case we expect that the density jump which bounds the flowing layers, $\delta\rho$, to be zero.

In the second case (C2, figure 3*c*), the two flowing layers touch at a single point. It can be shown that, for the self-similar flows considered here, if the layers are constrained to touch where their gradients are equal, then the curvature of the height reduction factor α ensures that the bounding streamfunctions of the active layers do not cross. This is analogous to Engqvist's solution with $\Delta h = 0$, and $\delta\rho$ finite. The inactive region still exists in this solution, and is of finite thickness throughout the length of the channel except for the point where the layers touch. Therefore, the criterion for stratified exchange discussed in the Appendix (that the dividing streamfunction either has a zero density gradient, or else can only occupy at one position in the vertical) is met for both cases C1 and C2.

The solution of these equations requires knowledge of the upstream withdrawal height h_i for each layer. We impose several restrictions which allow us to calculate these heights, namely that the two layers are closest at some non-dimensional width b_0' to be determined,

$$\alpha_1(b_0')h_1 + \alpha_2(b_0')h_2 = 1 - \Delta h \tag{2.17}$$

(where all heights have been non-dimensionalized by the total height H of the channel) at the point where their gradients are equal, that is

$$\frac{\mathrm{d}\alpha_1(b_0')}{\mathrm{d}b'}h_1 = -\frac{\mathrm{d}\alpha_2(b_0')}{\mathrm{d}b'}h_2. \tag{2.18}$$

https://doi.org/10.1017/S0022112003007171 Published online by Cambridge University Press

In addition there are conditions on the density of the streamlines bounding the active layers, namely

$$\text{C1}: \qquad \rho_1(h_1) = \rho_2(h_2), \qquad \delta\rho = 0, \tag{2.19a}$$

or

$$\text{C2}: \qquad \Delta h = 0, \qquad \delta\rho = \frac{\rho_2(h_2) - \rho_1(h_1)}{2}, \tag{2.19b}$$

where we have assumed that stagnant fluid has density which is the half-way between the densities on the streamline bounding either active layer.

One more condition on layer heights is required to close this problem. This condition, in keeping with previous solutions for internal hydraulic flows, is the necessity for a specified barotropic flux q_0 through the channel. This can be related to the individual layer fluxes via

$$q_0 = q_1 - q_2, \tag{2.20}$$

where the flux of each layer can be determined by integrating across the layer,

$$q_i = \int_0^{h_i} Q(\eta_i)\,\mathrm{d}\eta_i. \tag{2.21}$$

The method of solution for this flow is in two parts. The first is geometric, and solves for h_1 and h_2 as a function of the width where the two layers are closest, b_0'. Using (2.15), we obtain

$$\frac{\mathrm{d}\alpha}{\mathrm{d}b'} = \frac{2\alpha(1-\alpha)}{(3\alpha-2)b'} \tag{2.22}$$

so that

$$h_i = (1-\Delta h)\frac{(3\alpha_i - 2)(1-\alpha_{3-i})}{\alpha_i(\alpha_i - \alpha_{3-i})}, \quad i = 1, 2, \tag{2.23}$$

where the α_i are evaluated from (2.16) at b_0'. Figure 2(*b*) shows the h_i, apart from the multiplicative factor $(1-\Delta h)$, with the simple naming convention that h_2 is the bigger of the depths.

The second part of the solution (which will determine b_0', $\delta\rho$ and Δh) is typically iterative, since it involves the fluxes in the two layers and these depend on the density jump between the layers. In turn, these depend on the upstream heights h_i. Our approach is a straightforward iterative technique in which we aim to meet a specified target barotropic flux q_0^*:

(*a*) Guess an initial value for the position x_0 in the channel to give b_0'.

(*b*) Evaluate α_1 and α_2 at that position using (2.16).

(*c*) Assume case C2, so that $\Delta h = 0$, and use (2.23) to determine h_1 and h_2.

(*d*) $\delta\rho$ can then be determined from (2.19*b*). If $\delta\rho \geqslant 0$ then our assumption of case C2 was justified and we go to point (*f*). If $\delta\rho < 0$ then we have case C1.

(*e*) For case C1 we must iterate over successively larger values of Δh, each time evaluating the value of h_i from (2.23) until we satisfy the density condition $\rho_1(h_1) = \rho_2(h_2)$ given by (2.19*a*).

(*f*) Evaluate q_0 from (2.20) and (2.21). If the value of $q_\delta = q_0 - q_0*$ is smaller than a set tolerance, then exit the loop. Otherwise choose a new value of $x_0 = x_0 + \gamma q_\delta$ and return to point (*b*).

https://doi.org/10.1017/S0022112003007171 Published online by Cambridge University Press

3. Numerical model

The solution outlined above relies on the assumption that the flow in each layer is self-similar. We now test the theory (and, by implication, the self-similar assumption) by simulating stratified exchange flows with a hydrostatic two-dimensional numerical model. The model timesteps a density equation, which is obtained by integration across a channel of variable width (where v at the wall of the channel is found from u and the horizontal gradient in channel width), giving

$$b\frac{\partial \rho}{\partial t} = -b\boldsymbol{u}\cdot\nabla\rho + \nabla\cdot(b\boldsymbol{K}\cdot\nabla\rho). \tag{3.1}$$

The horizontal momentum equation is found in the same manner:

$$\frac{\partial u}{\partial t} = -\boldsymbol{u}\cdot\nabla u - \frac{1}{\rho_0}\frac{\partial p}{\partial x} + \frac{1}{b}\nabla\cdot(b\boldsymbol{A}\cdot\nabla u). \tag{3.2}$$

Variables are discretized on an Arakawa C-grid, and a leapfrog timestep system is used. We have used $\boldsymbol{u} = (u, w)$ as the velocity vector, with $\boldsymbol{K} \equiv (K_H, K_V)$ the diffusion coefficients and $\boldsymbol{A} \equiv (A_H, A_V)$ the viscosity coefficients. These coefficients are as small as numerically possible for the numerical resolution used; tests with finer resolution and correspondingly smaller coefficients have almost identical solutions to those shown here. Vertical velocity can be found from the divergence equation

$$b\frac{\partial w}{\partial z} = -\frac{\partial bu}{\partial x}, \tag{3.3}$$

and pressure from the hydrostatic relation

$$\frac{\partial p}{\partial z} = -\rho g. \tag{3.4}$$

The total barotropic flux is constrained by requiring that

$$\int_0^H u\,\mathrm{d}z = \frac{q_0}{b}, \tag{3.5}$$

at every point in the channel.

The model also includes a convection routine which acts to remove unstable stratification. This routine is computationally expensive, and so for many of the examples shown, convection is turned off, and unstable stratification is allowed to form. As shown below, this unstable stratification only occurs in regions where the fluid is inactive in the analytical solution, and we include a case (see §4.1.3) to demonstrate that convection plays only a minor role in setting the mean flow.

The model is non-dimensionalized to make b have a minimum value of 1, and g, ρ_0 to become unity. The boundary conditions are a rigid lid on the top and bottom ($w = 0$), with free slip ($\mathrm{d}u/\mathrm{d}z = 0$) and no flux ($\mathrm{d}\rho/\mathrm{d}z = 0$). The open boundaries at either end of the channel also have no vertical velocity ($w = 0$) and outward flow there satisfies a radiation condition. The density at the open boundaries is set by the pre-defined reservoir density profile when horizontal velocity is directed into the channel. In addition, the horizontal viscosity and diffusion are amplified close to the boundary to minimize reflection of internal waves.

The input parameters to the model include the width

$$b'(x) = 2 - \mathrm{sech}^2\left(\frac{3x}{L}\right), \tag{3.6}$$

https://doi.org/10.1017/S0022112003007171 Published online by Cambridge University Press

which is defined so that there is a simple minimum at $x = 0$. Density profiles at either end of the channel are prescribed, as well as the barotropic flux q_0, and the diffusion and viscosity coefficients. The model uses 300 gridpoints in the horizontal and the vertical, and is initialized with a zero velocity condition and a density field which smoothly connects the end density profiles. The model is run until a steady state is reached.

4. Comparisons

We now compare the numerical and analytical solutions, to determine whether the assumption of self-similarity and the derived solution provide a suitable description of stratified exchange flows. This is necessary because we cannot present a theoretical argument to fully justify the assumption of self-similar flow. Therefore, in comparing the two solutions we primarily investigate whether the self-similar solution is selected by the numerical simulation. We also compare the velocity and density distributions in the steady state, but note that we expect to see some differences due to the role of diffusion and viscosity, which is necessary in the simulations for numerical stability, but is explicitly excluded in the theory. Thus we anticipate that the numerical solution will be more diffuse, particularly close to the edge of the active layers, where discontinuities in velocity and density gradients are present in the analytical model.

In most cases presented, both reservoirs are linearly stratified with the same density gradient (described by the top to bottom density difference δ_V), but the mean density of each reservoir is offset by a small amount (the horizontal density difference being δ_H). The reservoir density profiles are

$$\rho_1 = \delta_V \eta_1 - \tfrac{1}{2}\delta_H, \tag{4.1}$$

$$\rho_2 = \delta_V (1 - \eta_2) + \tfrac{1}{2}\delta_H, \tag{4.2}$$

where we assume a channel height of $H = 1$. The ratio of vertical to horizontal density differences $r_\rho = \delta_V/\delta_H$ governs whether solution C1 or C2 will be selected. For large values of r_ρ the stratification in the reservoirs is strong and solution C1 is expected. For small r_ρ solution C2 is possible.

4.1. *Case C1*

4.1.1. *Linear stratification and zero barotopic flow*

We begin with an example with large r_ρ and zero barotropic flow. For this case we will demonstrate the method of solution and explicitly derive the solution. Since this case has zero barotropic flow, symmetry implies that the position x_0 where the layers are closest is at the centre of the channel; thus we can write the solution down without the iterative method outlined in § 2.2. In addition, equations such as (2.18) are not valid (since there is an implicit division by $\mathrm{d}b'/\mathrm{d}x$), so that we rewrite this equation as

$$\frac{\mathrm{d}\alpha_1(x_0)}{\mathrm{d}x} h_1 = -\frac{\mathrm{d}\alpha_2(x_0)}{\mathrm{d}x} h_2, \tag{4.3}$$

which implies that $h_1 = h_2$. Equation (2.17) can then be written

$$\tfrac{4}{3} h_i = 1 - \Delta h. \tag{4.4}$$

We need to establish whether this example belongs to case C1 or C2. Start by assuming case C2 so that $\Delta h = 0$. We then calculate from (2.19*b*), $\delta\rho = \delta_H(1 - r_\rho/2)/2$, implying an unstable density gradient in the analytical solution when $r_\rho > 2$. Case C1

https://doi.org/10.1017/S0022112003007171 Published online by Cambridge University Press

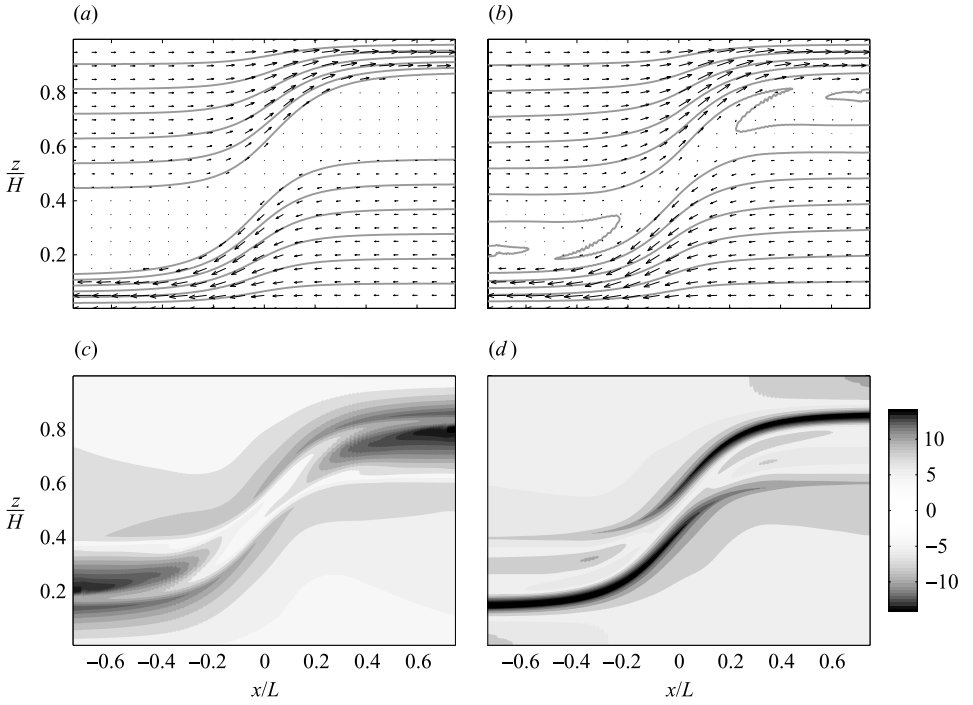


FIGURE 4. Engqvist's solution (case C1) with $r_\rho = 4$ and $q_0 = 0$. (*a*) Isopycnals (contours) and velocity (vectors) for the self-similar analytical solution; (*b*) isopycnals and velocity for numerical simulations; (*c*) difference in density (numerical − analytical) expressed as a percentage of the density range; (*d*) difference in horizontal velocity (numerical − analytical) expressed as a percentage of the velocity range.

will be selected when this condition occurs, so that $\delta\rho = 0$; we find $\Delta h = 1/6$ and $h_1 = h_2 = 5/8$. Knowledge of the withdrawal heights and height reduction factors everywhere allows us to compute density in the channel as a function of position. It remains to calculate the reservoir Bernoulli function for each layer which we do by integrating (2.5) which, for the case of the lower layer, gives

$$B_{\infty 2} = -\tfrac{1}{2}\delta_V \eta_2^2 + E. \tag{4.5}$$

The constant E can be found from the upper boundary condition (2.9) which for the case of $\delta\rho = 0$ trivially gives

$$E = \tfrac{1}{2}\delta_V h_2^2, \tag{4.6}$$

so that

$$B_{\infty 2} = \tfrac{1}{2}\delta_V \left(h_2^2 - \eta_2^2\right) \tag{4.7}$$

can be used to give velocities everywhere in the lower layer using (2.13). The same procedure can be used to give upper-layer velocities. Note that the self-similar solution involves a velocity profile which depends nonlinearly on height both in the reservoir and in the channel.

The resulting flow is shown in figure 4(*a*) for the case $r_\rho = 4$, with velocity indicated by the vectors and density by contours. The numerical simulation, shown in panel (*b*), appears to be qualitatively similar. Both solutions show antisymmetric layers which accelerate through the contraction. The layers show no sign of interaction, as a region of zero (or small) velocity divides the two flowing layers. The two lower panels in this

https://doi.org/10.1017/S0022112003007171 Published online by Cambridge University Press

diagram show the differences between the numerical and analytical solutions for the density (c) and velocity (d) fields. The differences are measured as a percentage of the range in density and velocity respectively. Importantly, these diagrams show that, to first order, the assumption of self-similarity applies in the numerical solution. Within the active layers the differences between the two solutions are generally very small (<3%). Self-similarity deteriorates with distance along the channel, which is expected from the impact of diffusion and viscosity on the numerical solution.

The largest differences between the numerical and analytical solutions can be seen at the edge of the flowing layers, and within the inactive regions. Differences in the velocity field are as high as 10%–15%. It is worthwhile noting that the analytical solution predicts a discontinuity in the velocity gradient at this point, so that the diffusive flux in the numerical solution is expected to be large. Viscosity thus acts to thin the stagnant region in the centre of the channel (near $x/L = 0$) so that it might appear from the numerical solution that the stagnant region does not extend to the centre of the channel. In addition, viscosity causes a recirculating cell to form at the ends of the channel. The velocities in this region are small compared to velocities in the active layers, but the effects of recirculation can be seen in the density field. In fact, the largest errors in the density field are due to these recirculations, which produce a statically unstable density profile in the inactive parts of the flow. These unstable regions are allowed to develop, as the convection routine is turned off (see § 3). It is shown in § 4.1.3 that the addition of convection removes the unstable density fields without altering flow in the active layers.

The case shown in figure 4 confirms that the self-similar solution for stratified exchange flow derived here is physically plausible. We now show a number of cases to demonstrate that this result is robust. The next example (figure 5) is a case with $r_\rho = 2$ which is on the boundary between cases C1 and C2: this example yields Engqvist's solution with $\Delta h = 0$, or equivalently case C2 with $\delta\rho = 0$. There is a stagnant layer separating the two active layers at all points except the centre of the channel. The thickness of the stagnant layer depends only upon $\alpha(b)$. As above, self-similarity applies within the flowing layers to within approximately 3%. The errors in the velocity field are largest at the layer boundaries, and recirculation produces a density inversion where we expect stagnant regions. In short, there is no additional evidence in figure 5 which would indicate that the self-similar solution will not apply here.

4.1.2. *Finite barotopic flux*

We now add the complication of finite barotropic flow rate to the models, and present solutions for a case with Engqvist's solution (figure 6) with $r_\rho = 4$ and $q_0 = 0.1$. The first-order effect of adding the barotropic flow is to move the point where the layers are closest to a position upstream relative to the barotropic flow direction. This feature is observed in the numerical and analytical solution for the case shown here, where $x_0 = -0.11$. Otherwise, the simulation shows similar trends to the cases described above. Differences between simulations and predictions are large at the edge of the flowing layers and in the stagnant regions due to viscosity and diffusion, and are small in the active layers. Self-similarity is preserved to within 10% in the layers, which is a larger error than in the zero barotropic flow examples above. This evidence demonstrates that self-similar stratified solutions provide a good approximation of the observed flow field, and that the self-similarity seen in other cases is not simply due to symmetrical flow in the two flowing layers.

https://doi.org/10.1017/S0022112003007171 Published online by Cambridge University Press

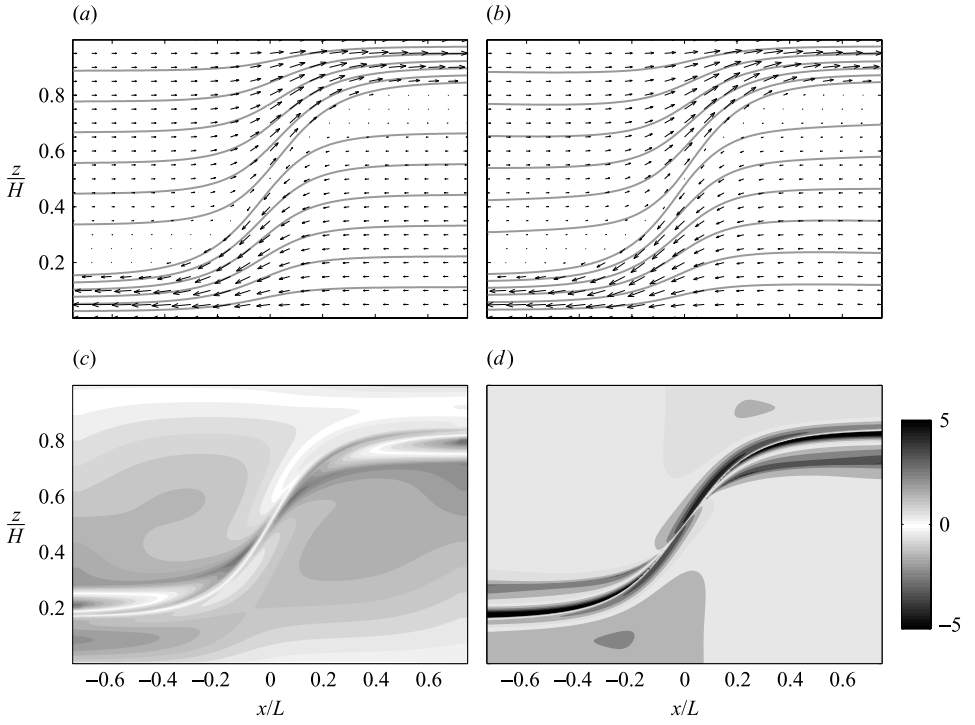


FIGURE 5. As figure 4 but for a case with both $\Delta h = 0$ and $\delta\rho = 0$ using $r_\rho = 2$ and $q_0 = 0$.

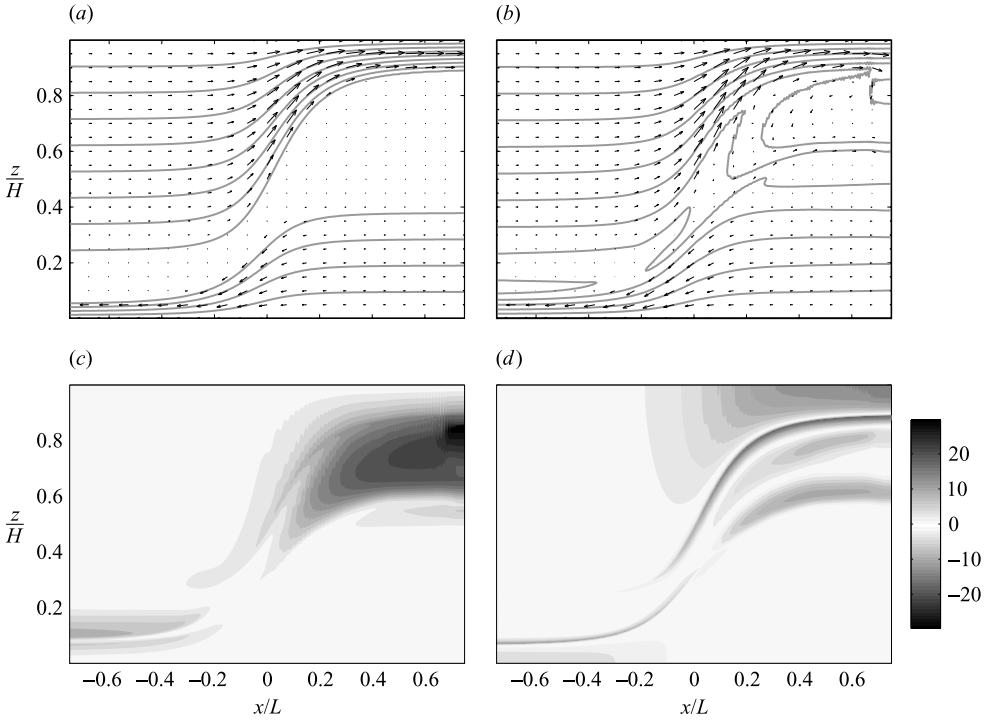


FIGURE 6. As figure 4 but for Engqvist's solution (C1) with finite barotopic flow rate. $r_\rho = 4$ and $q_0 = 0.1$. The two layers are closest at $x_0 = -0.11$ in the analytical solution.

https://doi.org/10.1017/S0022112003007171 Published online by Cambridge University Press

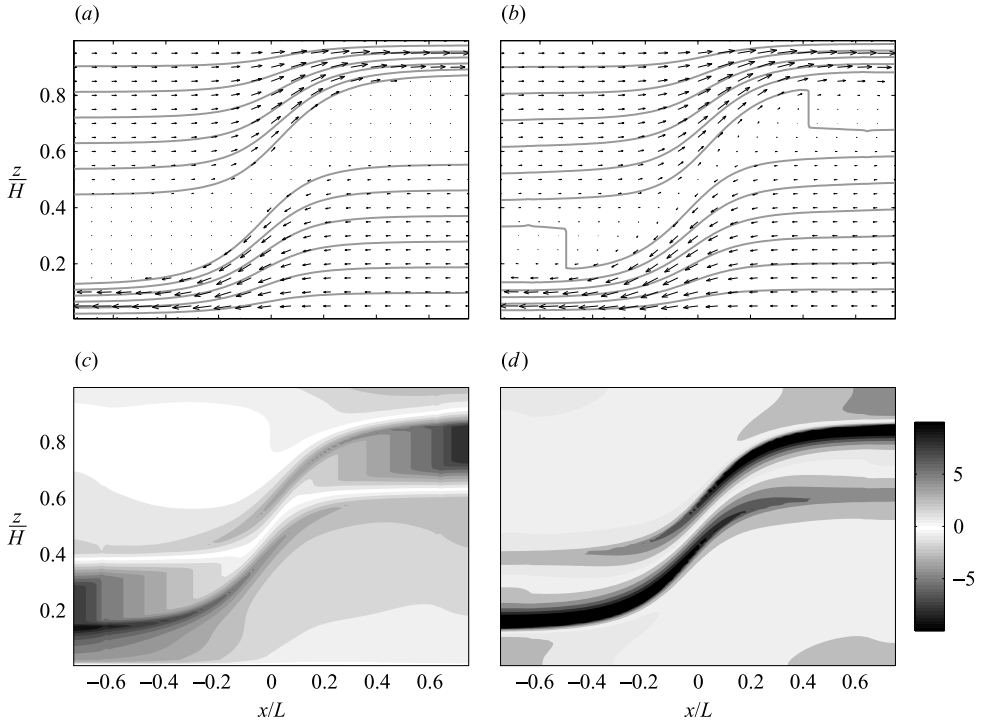


FIGURE 7. As figure 4, but with the convection routine turned on. Note that resolution was lowered to 100×100 for this case.

4.1.3. *Convection*

The unstable convection which develops in the numerical solutions shown above is acknowledged to be unrealistic, and can be avoided using a simple convection routine. However, the numerical algorithm which calculates convection is slow, so that it is impractical to run cases at high resolution with the convection switched on. We now show a case with the resolution reduced by a factor of 3 and convection active, to demonstrate that the addition of convection does not significantly change the simulation. The difficulty we face here is that in lowering resolution we must increase viscosity and diffusion, so that in figure 7, which uses a simulation with the same parameters as figure 4, the impact of viscous effects is greater. However, the numerical simulation shows all those features that we observed in the original case, with small errors within the active layers and large errors elsewhere. This indicates that the results described above are insensitive to convection in the inactive regions of the flow.

4.2. *Case C2*

4.2.1. *Linear stratification and zero barotropic flow*

A more stringent test of the self-similarity assumption is the case where stratification is further weakened, as shown in figure 8, so that the analytical solution requires that the layers meet at a point and the density jump $\delta\rho$ is finite. The implication of this solution is that some fluid from (say) reservoir 2 is dense enough that it might be exchanged, but that the requirement for self-similar flow, in combination with the existence of flow in layer 1, acts to block the passage of this dense fluid. The data shown in figure 8 support the hypothesis that self-similar flow occurs in this case.

https://doi.org/10.1017/S0022112003007171 Published online by Cambridge University Press

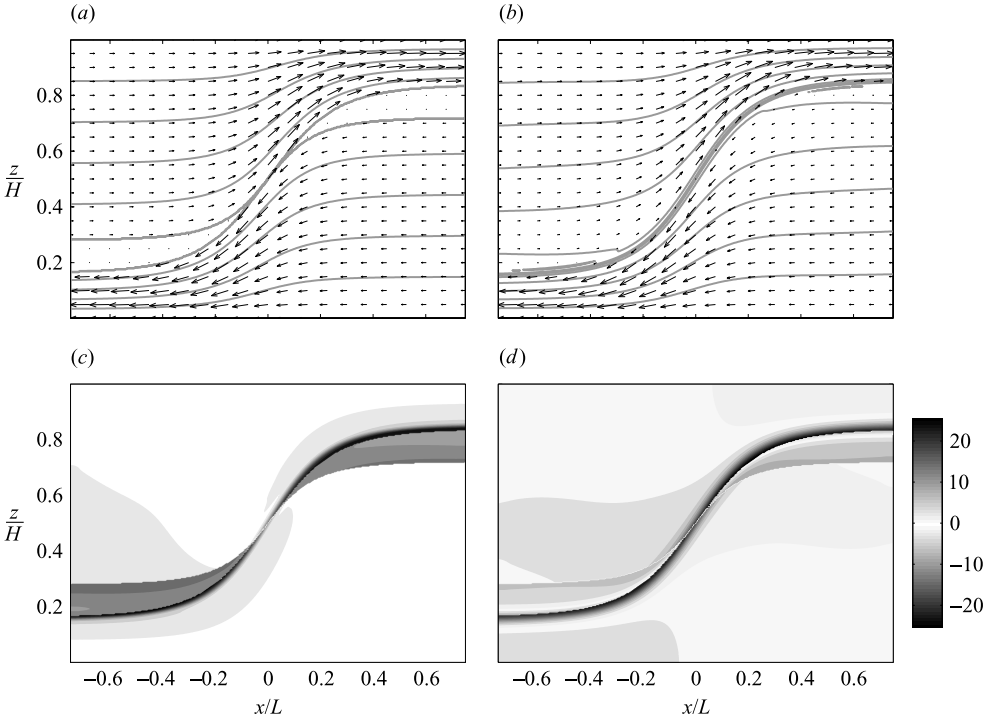


FIGURE 8. As figure 4 but for case C2 using $r_\rho = 1$ and $q_0 = 0$.

This can be seen by the small differences (<5%) within the two flowing layers. In this case there are discontinuities in both density and velocity at the edges of the flowing layers in the analytical solution. The result is that diffusion is large in the numerical solution so that differences between numerical and analytical predictions are as great as 20% at the edges of the layers. In this case the errors produced by diffusion exceed those due to recirculation in the inactive regions. Viscosity also acts to reduce the total transport of each layer. This occurs because viscosity reduces the effective height of the layers at the control point, so that the layer heights are slightly smaller than the theoretically predicted thickness.

The analytical solution in figure 8 includes a finite-width stagnant region everywhere except at $x = 0$. However, the numerical solution (figure 8*b*) shows that the stagnant region is only observable there towards either end of the channel. This highlights the role of viscosity in thinning the stagnant region. One can infer from these simulations, which use the minimum viscosity necessary for stability, that stagnant layers are unlikely to be observed in geophysical flows with reasonable values of viscosity. Nonetheless, the importance of self-similarity in the simulated flow indicates the relevance of the solution presented here as an estimate of exchange flux.

4.2.2. *Finite barotropic flux*

The results for case C2 with a large barotropic flow rate are shown in figure 9, which demonstrates that the difference between simulation and theory in this case is greater than shown previously; as great as 15% within some of the layers. These discrepancies are seen in other C2 cases with strong barotropic flows (not shown) and the mismatch becomes more pronounced as barotropic flow is increased. It was shown in §4.1.2 that case C1 with strong barotropic flow also showed greater discrepancies

https://doi.org/10.1017/S0022112003007171 Published online by Cambridge University Press

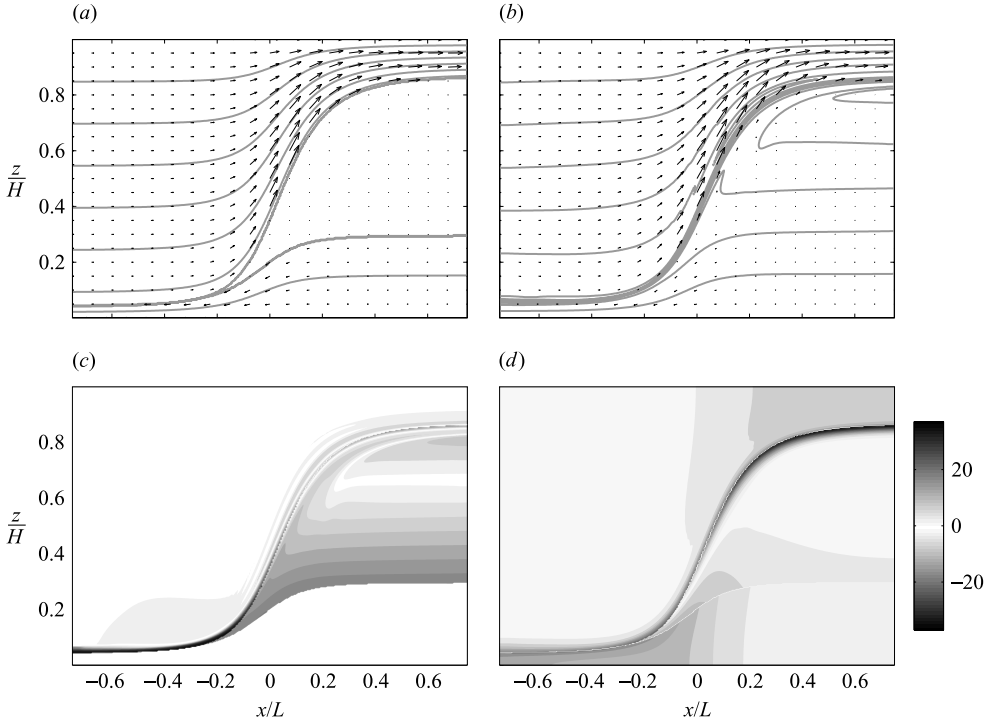


FIGURE 9. As figure 4 but for case C2 with finite barotropic flow rate, $r_\rho = 1$ and $q_0 = 0.2$. In the analytical solution the layers touch at $x_0 = -0.36$.

between theory and simulation. These results may indicate that self-similarity does not hold in all cases, or alternatively that the production of thinner layers and strong shear in parts of the channel when barotropic flow is introduced are responsible for the discrepancy. We have no way of distinguishing between these possibilities and thus conclude that, while the self-similar theory gives a good approximation of the observed viscous flow, we are unable to prove the validity of the self-similar solution in all cases shown.

4.2.3. *Nonlinear stratification*

The examples shown so far demonstrate the viability of the self-similar solution over a range of conditions. It is notable, however, that in each case stratification in the reservoirs is linearly dependent upon depth. We now relax this condition and show results from an exchange flow where the left-hand reservoir has a quadratic stratification. The results for this case are shown in figure 10 using the same format as results in the previous subsections.

One difference between the flows shown in this case and the previous cases is that the point where the layers are closest (x_0) is found to the right of the contraction, even though the barotropic flux is set to zero. This asymmetry is a function of the asymmetry of the flow: the two active layers no longer have the same vertical profile of velocity. This profile is a function of the density, and therefore the upper part of layer 1 has higher velocity than the lower part of layer 2. Nonetheless, the observed differences between the numerical and analytical solutions again support the notion of self-similarity. An extra feature of the nonlinear stratification is that diffusion is now non-zero within the layers. Despite this, differences between the two solutions

https://doi.org/10.1017/S0022112003007171 Published online by Cambridge University Press

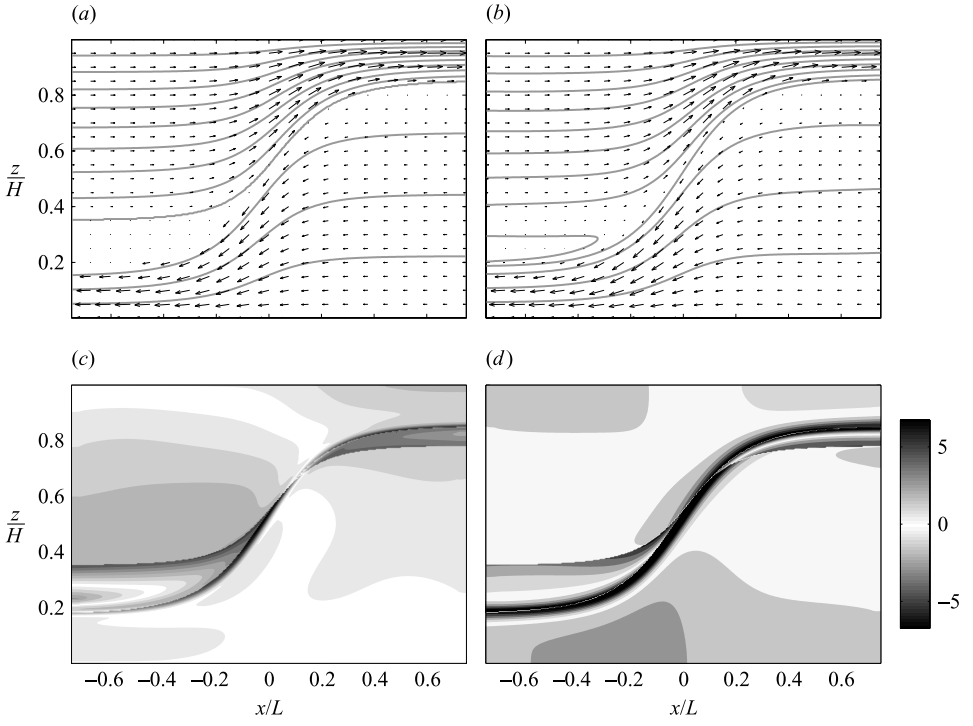


FIGURE 10. As figure 4 but for a case with nonlinear stratification in the left-hand reservoir. $\rho_1 = -0.3\eta_1^2 + 0.8\eta_1 - 0.4$, $\rho_2 = 0.2(1 - \eta_2)$ and $q_0 = 0$.

show that in the active part of the flow errors are lower than 3%. Large differences are seen at the edges of the layers as in previous cases. We conclude from this evidence that the addition of nonlinear stratification does not alter the applicability of the self-similar solution.

5. Discussion

We have presented a method of calculating flow between stratified reservoirs assuming that flow within each of two active layers is self-similar. The simplification yielded by the assumption of self-similarity allows us to solve analytically for flow in both layers, producing a solution which predicts that parts of the fluid column are inactive. It is these inactive or stagnant regions which allow us to overcome the paradox raised by Killworth (1992). In that paper it was shown that if bi-directional stratified exchange flow were to occur, then the zero-velocity streamline can only occupy one vertical position. The self-similar solutions bypass this condition because the zero streamline(s) occur in regions of the flow where there is no vertical gradient in density.

We have proposed two self-similar cases which are solutions for stratified bi-directional flow through a flat-bottomed contracting channel. Confirmation of the solutions is difficult. The theory described here is inviscid by necessity, and yet we are using it as a theoretical model to describe flows which will always feel the effect of viscosity. This is true for observed geophysical flows, laboratory models and numerical simulations. Numerical simulation allows the greatest scope for comparison, since we can run the model such that viscosity and diffusion are minimized. These comparisons

https://doi.org/10.1017/S0022112003007171 Published online by Cambridge University Press

show the first-order effect that viscosity and diffusion have upon the flow, and that the major elements of the theoretical solution can be identified in the simulated flows.

For case C1 the condition of self-similarity appears to be retained in the simulations. The major differences between the simulated and theoretical solutions can be seen at the edges of the active regions where there are discontinuities in velocity and density gradients, and in the inactive regions where a residual viscosity-driven circulation can be identified in the numerical simulations. Discrepancies are larger when there is a finite barotropic throughflow. We conclude that the self-similar solution C1 may be a solution for inviscid stratified exchange flows in the limit of strong reservoir stratification, and can be used as a first-order prediction for flow in the viscous case.

In all of the C1 examples shown, the inactive regions are thinned by the transfer of momentum from the neighbouring active layers. This acts to mask the existence of the stagnant regions in the viscous case, and provides an explanation as to why the self-similar solution to stratified exchange flows has not been considered before as a general solution to this problem. There is unlikely to be any observational evidence indicating that a stagnant region plays a role in dynamic flows. This does not reduce the relevance of the inviscid solution as a tool for estimating flow in the viscous case.

The evaluation of the validity of case C2 is complicated by the grater role played by viscosity and diffusion in the simulations. It was observed that discrepancies increase with increasing barotropic flow rate, which may be due to the increased role of viscosity in simulations with thin layers and strong shear, or alternatively to the breakdown of the self-similar solution in such cases. Nonetheless, in cases with small barotropic flow rate the C2 solutions provide a good estimate of flux of density through the contraction.

It is interesting to extend the self-similar solution to the two-layer case. This is analogous to the C2 solution in the limit $r_\rho \to 0$. To do this we need to replace the upper boundary condition (2.9), which becomes invalid when the density gradient ρ_η is zero. The new condition is simply

$$B(h) = \frac{\delta\rho g h}{\rho_0}, \tag{5.1}$$

and we note that with no density gradient B does not vary with height, so that

$$B_\infty = \tfrac{1}{2} g' h. \tag{5.2}$$

Here we have introduced the reduced gravity g', and to maintain consistency with the two-layer hydraulic literature have defined

$$g' \equiv \frac{2\delta\rho g}{\rho_0}. \tag{5.3}$$

It follows that we can now compute the velocity at any point in the channel from (2.13) to give

$$u = \sqrt{g' h (1-\alpha)}. \tag{5.4}$$

We then define the Boussinesq composite Froude number from Armi (1986),

$$G^2 \equiv \frac{u_1^2}{g' d_1} + \frac{u_2^2}{g' d_2} \tag{5.5}$$

where d_i is the local layer depth. We can rewrite the composite Froude number as

$$G^2 = \frac{1-\alpha_1}{\alpha_1} + \frac{1-\alpha_2}{\alpha_2}, \tag{5.6}$$

https://doi.org/10.1017/S0022112003007171 Published online by Cambridge University Press

so that at the contraction, where $\alpha = 2/3$ in both layers, the critical condition ($G^2 = 1$) applies. It can then be easily shown that the self-similar solution gives the same prediction for flux in the layers for the case with zero barotropic flow, although the details of the flow field away from the contraction differ due to stagnant regions in the self-similar solution. In cases with a finite barotropic throughflow, the critical condition is still met in both layers at the contraction; however, a finite-thickness stagnant region is present there, producing a different solution from that obtained by two-layer hydraulics.

The failure of the C2 solution to merge smoothly with the two-layer solution at finite barotropic flow rate lends further weight to the argument that C2 is not an exact solution to stratified exchange flows. This raises the possibility that the true solution is one where the two active layers are in contact over a finite distance. Such a solution would not be everywhere self-similar, although each active layer may be self-similar upstream of the point where the layers merge. An additional constraint is required for a solution where layers are coupled over some distance; it is possible that the merging point will occur at the mode 2 virtual control point (see the discussion in the following paragraph for details), and that upstream of this point the active layers, separated by a stagnant region, are self-similar. Any such solution will require additional theoretical development and testing beyond the scope of this paper.

This paper demonstrates the conditions under which self-similar exchange flow can be used to predict flow through a contraction in a channel, given only the two reservoir stratifications and the net (barotropic) throughflow. There are a large number of questions regarding this problem which remain unanswered. For example, why is the self-similarity solution selected in these cases? This issue was addressed partially by Benjamin (1981) and Armi & Williams (1993), and relates to virtual controls of high internal wave modes. As fluid in the active layers approaches the contraction it is accelerated through a succession of virtual controls at which the flow becomes critical with respect to first mode ∞ and finally mode 2 internal waves (see Engqvist 1996 for a full discussion of virtual controls in the layered exchange flow solution). By examining solutions 'close' to the similarity solution, Armi & Williams (1993) found that such solutions only exist at virtual controls (and found no other solutions away from virtual controls). Thus, perturbed self-similar solutions could not smoothly connect reservoir densities to the topographic control point (Benjamin 1981). It is implied that only self-similar solutions can pass through the virtual controls, and provides some justification for the apparent strong constraint of self-similarity on exchange flows simulated here. However, the general question of whether there are other solutions which can pass through the successively more frequent virtual controls (as the channel becomes wider) remains unanswered.

The stagnant layers which are specified in these analytical solutions present two difficulties. Firstly there is the question of how they form, and secondly how they connect to reservoir conditions. The former question presents little difficulty for case C1, where the stagnant layer is constrained in density by the fact that the bounding densities of the two active layers are equal. However, for case C2 we have (somewhat arbitrarily) chosen the stagnant layers to have density which is intermediate between the two bounding densities. It is important to stress that this density cannot be achieved by mixing in our inviscid solution. We have chosen this density as a suitable boundary condition on the active layers which allows computation of the solution. The simulations indicate that in a time-dependent flow the actual density of the stagnant layers may vary without greatly altering the flow.

https://doi.org/10.1017/S0022112003007171 Published online by Cambridge University Press

Similarly, it is not possible for the homogeneous stagnant layers to connect smoothly to reservoir densities in a time-dependent flow for either cases C1 or C2. A possible scenario is shown in figure 7 for the case in which convection is included. This produces a horizontal gradient in density within the stagnant layer. One might expect this to alter the solution to some extent; however, in hydraulically controlled flows such as these the solution is controlled at the throat of the contraction, so that the most relevant quantity is the density which acts as a boundary condition on the active layers there. For this reason the assumed homogeneous stagnant layers produce a solution which closely approximates the time-dependent cases.

It may also be noted that the fast flowing layers do not match reservoir conditions. In realistic flows it would be expected that a transition to subcritical flow (probably via an internal hydraulic jump) would occur. We have omitted this possibility by ignoring hydraulic jumps in the analytical solution, and by setting the boundary conditions at the open boundaries of the numerical solution to allow supercritical flow to pass out of the model domain. Internal hydraulic jumps may well occur in more realistic flows; however, the presence of stagnant layers means that the jump is insulated from altering the neighbouring active layer.

Despite these unresolved issues, the solutions presented here provide a simple resolution to a problem which has been assumed in the past to be too complicated to address. The solutions give useful and simple estimates for flux through a contraction in a channel between stratified reservoirs, and the problem can be solved analytically. It is not clear how to extend this solution to other geometries, for example channels with varying topography where a sill provides the topographic control rather than a contraction, since no similarity solution is available in such cases (cf. Killworth 1992, for a numerical non-similar solution).

We are indebted to Larry Armi who pointed out errors in our original formulation. Our thanks also to David Smeed and Harry Bryden for providing us with comments on the first draft of this manuscript. Two anonymous referees also assisted in improving the paper.

Appendix. Flow behaviour at a dividing streamline

We consider briefly the possible solutions at a point $u = 0$ in a quasi-two-dimensional flow of ideal fluid described by

$$(bu)_x + bw_z = 0, \tag{A 1}$$

$$u\rho_x + w\rho_z = 0 = bu\rho_x + bw\rho_z, \tag{A 2}$$

$$p_z = -g\rho, \tag{A 3}$$

$$uu_x + wu_z = -\frac{p_x}{\rho_0}. \tag{A 4}$$

We assume that somewhere at each vertical there is a point at which u changes sign. Thus

$$z = z_0(x),\ u = 0 \quad \text{at some level.} \tag{A 5}$$

The surface is denoted by C. Density is constant on C as it is a streamline; its value is denoted by $\hat{\rho}$. Thus

$$\rho(x, z_0(x)) = \hat{\rho}. \tag{A 6}$$

Differentiation of (A 6), if there are no infinite gradients, gives

$$\rho_x + z_{0x}\rho_z = 0 \text{ on C}. \tag{A 7}$$

At the level of zero horizontal flow, ρ_x may be finite or infinite.

https://doi.org/10.1017/S0022112003007171 Published online by Cambridge University Press

We assume first that ρ_x is finite. Then at least one of w and ρ_z must vanish on the surface where u vanishes, from (A 2). If w vanishes there, then (A 4) implies $p_x = 0$. Differentiating (A 4) with respect to z gives $\rho_x = 0$ on C. From (A 7), either z_{0x} or ρ_z must vanish on C. If z_{0x} vanishes, the Killworth (1992) solution is obtained, in which the surface C is everywhere flat, but there is a non-zero stratification across it. If, however, ρ_z vanishes on C, then all of u, w, ρ_x and ρ_z vanish on C, giving a locally stagnant region which is vertically unstratified exactly at the surface C.

The second possibility is that ρ_z vanishes on C but w does not. In such a case, (A 7) implies that ρ_x vanishes; indeed, provided w is indeed non-zero it is possible to show by repeated differentation that every derivative of density vanishes on C, a pathological case.

Thus, provided there are no infinite gradients in density, there are essentially two solutions for the surface C: (*a*) the surface is everywhere flat, with $u = w = \rho_x = 0$, $\rho_z \neq 0$; or (*b*) the surface is not flat, but $u = w = \rho_x = \rho_z = 0$ and the region is locally stagnant and unstratified. The remaining cases include the possibility of density jumps, when derivatives cannot be taken. These cannot, of course, be ruled out for an ideal fluid.

REFERENCES

Armi, L. 1986 The hydraulics of two flowing layers with different densities. *J. Fluid Mech.* **163**, 27–58.

Armi, L. & Farmer, D. M. 1986 Maximal two-layer exchange through a contraction with barotropic net flow. *J. Fluid Mech.* **164**, 27–51.

Armi, L. & Farmer, D. M. 1987 A generalization of the concept of maximal exchange in a strait. *J. Geophys. Res.* **92**, 14679–14680.

Armi, L. & Williams, R. 1993 The hydraulics of a stratified fluid flowing through a contraction. *J. Fluid Mech.* **251**, 355–375.

Baines, P. G. 1988 A general method for determining upstream effects instratified flow of finite depth over long two-dimensional obstacles. *J. Fluid Mech.* **188**, 1–22.

Benjamin, T. B. 1981 Steady flows drawn from a stably stratified reservoir. *J. Fluid Mech.* **106**, 245–260.

Dalziel, S. B. 1991 Two layer hydraulics: a functional approach. *J. Fluid Mech.* **223**, 135–163.

Engqvist, A. 1996 Self-similar multi-layer exchange flow through a contraction. *J. Fluid Mech.* **328**, 49–66.

Helfrich, K. L. 1995 Time-dependent two-layer hydraulic exchange flow. *J. Phys. Oceanogr.* **25**, 359–373.

Hogg, A. M., Ivey, G. N. & Winters, K. B. 2001 Hydraulics and mixing in controlled exchange flows. *J. Geophys. Res.* **106** (C1), 959–972.

Killworth, P. D. 1992 On hydraulic control in a stratified fluid. *J. Fluid Mech.* **237**, 605–626.

Lane-Serff, G. F., Smeed, D. A. & Postlethwaite, C. R. 2000 Multi-layer hydraulic exchange flows. *J. Fluid Mech.* **416**, 269–296.

Lawrence, G. A. 1990 On the hydraulics of Boussinesq and non-Boussinesq two-layer flows. *J. Fluid Mech.* **215**, 457–480.

Smeed, D. A. 2000 Hydraulic control of three-layer exchange flows: Application to Bab al Mandab. *J. Phys. Oceanogr.* **30**, 2574–2588.

Winters, K. B. & Seim, H. E. 2000 The role of dissipation and mixing in exchange flow through a contracting channel. *J. Fluid Mech.* **407**, 265–290.

Wood, I. R. 1968 Selective withdrawal from a stably stratified fluid. *J. Fluid Mech.* **32**, 209–223.

Wood, I. R. 1970 A lock exchange flow. *J. Fluid Mech.* **42**, 671–687.

Yih, C.-S. 1969 A class of solutions for steady stratified flows. *J. Fluid Mech.* **36**, 75–85.

Zhu, Z. & Lawrence, G. A. 1998 Non-hydrostatic effects in layered shallow water flows. *J. Fluid Mech.* **355**, 1–16.

https://doi.org/10.1017/S0022112003007171 Published online by Cambridge University Press